MINEROLOGICAL JOURNAL, VOL. 14, NO. 1, PP. 1–11, JANUARY 1988.

Anisotropic etching and annealing of fission tracks in quartz

A.S. SANDHU, SURINDER SINGH and H.S. VIRK

Department of Physics, Guru Nanak Dev University, Amritsar 143005, India.

Abstract

The studies of each pit formation of fission fragment tracks in natural quartz are carried out using KOH, as the track etchant. The influence of crystallographic structure on the bulk etch rate, V_G, the track etch rate V_T, and the etching efficiency, η is reported. The value of fission track age is found to be the same for all the planes. It is observed that the annealing augments anisotropy of track revelation in the crystal. The activation energy, E_a, is found to vary with the crystallographic orientation.

Introduction

Since it has been introduced in 1963 (Price and Walker, 1963) the fission-track (FT) method has become widely used for dating various minerals and rocks. Several studies (Davie and Durrani, 1978; Gleadow, 1978; Green and Durrani, 1977; Singh *et al.*, 1986 and Sandhu *et al.*, 1987a) have been made of the etching and annealing behaviour of fission tracks in natural crystals. In most of the track etch work simple detectors like glasses and plastics are generally used which are isotropic. In fission track dating however, there is no choice but to use the natural detectors available in the form of uranium bearing minerals (Gleadow, 1978). Most of these minerals are anisotropic and are expected to have complicated track etching and annealing characteristics. This anisotropic behaviour can effect the fission track age of the minerals (Singh *et al.*, 1986). The anisotropic effect was first shown by Gegugin *et al.*, (1968) in muscovite mica and subsequently reported by Green and Durrani (1977) in apatite. Durrani *et al.* (1974) have examined the effect of anisotropic bulk etch rate in meteorite studies using bronzite and feldspar. Gleadow (1978) has reported work on track etch anisotropy in natural sphene.

In a recent publication (Sandhu *et al.*, 1987a), the authors have reviewed the evidence of the influence of crystallographic structure on annealing of fission tracks in apatite. In the present investigations an attempt is made to study the anisotropic track etching and annealing behaviour in natural quartz collected from Parbati Valley, Kullu district, Himachal Pradesh (India). In this area, the prominent rock types are quartzite, schist and gneisses.

Since the thermal conductivity, dielectric constant, electrical resistivity and hardness of quartz vary from plane to plane (Frondel, 1962), it follows that etching and annealing behaviour of fission tracks might be different for tracks in different orientations.

Experimental procedure:

1. Sample preparation:

The quartz used in the present study is a large crystal having about 7x2 cm^2 as the area of the crystal surface. The crystal structure of quartz is based on a hexagonal lattice. The quartz under study is colorless and transparent. The following crystal planes are taken for study:

a) The plane parallel to c-axis i.e. the prism m $\{10\bar{1}0\}$.
b) The plane inclined to c-axis i.e. the rhombohedra r $\{10\bar{1}1\}$ and z $\{01\bar{1}1\}$.
c) The plane perpendicular to c-axis i.e. the basal pinacoid $\{0001\}$.

Different samples of each plane were separated and prepared for grinding and polishing as described elsewhere (Singh *et al.*, 1984).

2. Standardisation of etching conditions:

In order to determine the optimum etching time for fission tracks in quartz, the samples of each plane were irradiated with ^{252}Cf fission fragment source in 2π geometry (by placing the samples in direct contact with the source) for 15 min each. These irradiated samples were then etched in 15 N KOH, at 125℃ for various time intervals ranging from 2 to 14 hrs. The tracks were then counted under an optical microscope at a magnification of 600x using a calibrated ocular graticule provided in the microscope. The results are shown in Fig. 1.

3. Measurement of track etch rate (V_T), bulk etch rate (V_G) and etching efficiency (η) on different planes:

a) Measurement of track etch rate (V_T):

The fission fragments from ^{252}Cf source were allowed to pass through a collimater (circular slit) of 0.5 mm diameter in a vacuum chamber ($\sim 10^{-3}$ atm.), so that a parallel beam of fission fragments may be achieved. Then, samples from each plane were irradiated at $15 \pm 2°$ angle of incidence.

These samples were then etched simultaneously in 15 N KOH at 125℃ for various time intervals ranging from 2 to 14 hrs. The mean track lengths (The observed projected length corrected by using angle of dip of the track in the detector surface) were measured at each time using an optical microscope at a magnification 1500x (Fig. 2). These measurements were made using a calibrated ocular scale provided in the microscope and twenty tracks were taken for observations. The track etch rate, V_T,

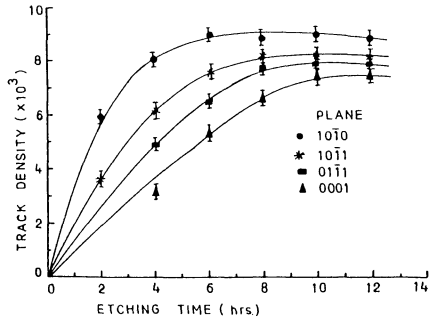

FIG. 1. The optimum etching time curve for fission tracks in quartz.

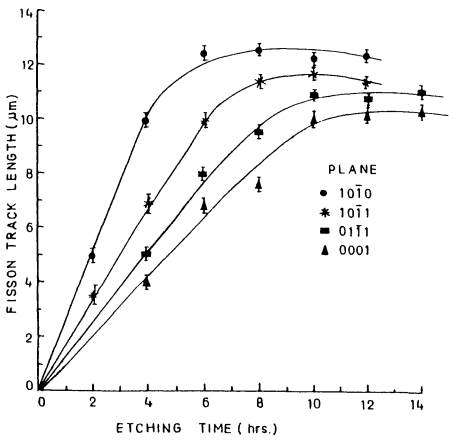

FIG. 2. The variation of track length (corrected for dip) with etching time for different planes of quartz.

was calculated from the slope of the linear portion of the plot of track length versus etching time (Fleischer *et al.*, 1975; Sandhu *et al.*, 1986).

b) Measurement of bulk etch rate (V_G):

Samples from each plane were irradiated at 90° angle of incidence with a parallel beam of fission fragments from ^{252}Cf source. After exposure, these samples were etched in 15 N KOH at 125℃ for various times ranging from 2 to 14 hrs and the track diameter was measured at each time interval. The bulk etch rate V_G, was calculated from one half of the slope of the curve etching time versus track diameter (Fig. 3) (Fleischer *et al.*, 1975; Singh *et al.*, 1986).

c) Measurement of η and θ_c:

The etching efficiency (η) and critical angle (θ_c) were calculated from the following relations (Fleischer *et al*, 1975; Sandhu *et al.*, 1986):

$$\eta = 1 - \frac{V_G}{V_T} \qquad (1)$$

or $\eta = 1 - \sin \theta_c$

or $\theta_c = \sin^{-1}(1 - \eta)$ (2)

The values of V_T, V_G, η and θ_c are reported in Table 1.

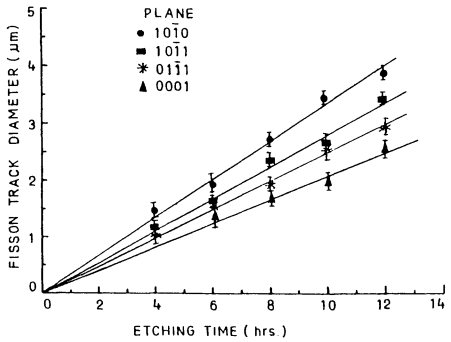

FIG. 3. The variation of track diameter with etching time for different planes of quartz.

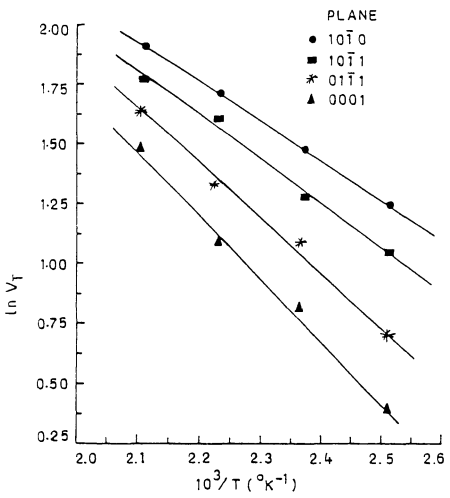

FIG. 4. Plot of ln V_T vs 1/T for different planes of quartz.

TABLE 1. The values of V_T, V_G, η, θ_c, E_T and E_a for different planes of quartz crystal.

Plane	V_T (μm/hr)	V_G (μm/hr)	η (%)	θ_c	E_T (eV)	E_a (eV)
10$\bar{1}$0	2.7	0.16	94.1	3.4°	0.143	1.73
10$\bar{1}$1	1.7	0.14	91.8	4.7°	0.162	1.44
01$\bar{1}$1	1.3	0.12	90.8	5.3°	0.195	1.27
0001	1.1	0.11	90.0	5.7°	0.221	1.15

4. Measurement of activation energy for track etching, E_T:

Four samples from each plane were irradiated with a parallel beam of ^{252}Cf fission fragment source in vacuum at 15 ±2° angle of incidence. These samples were then etched in 15 N KOH at 125°C, 150°C, 175°C and 200°C for various time intervals. The track etch rate V_T was calculated for each plane as discussed in section 3 a. The track etch rate, V_T, is exponential and may be expressed as:

$$V_T = A\, e^{-E_T/kT} \qquad (3)$$

where k, is the Boltzman constant, T, temperature (°K); and E_T, activation energy. The value of E_T, was calculated from the slope (Fig. 4) and is given in Table 1.

5. Angular distribution of etched tracks:

Two samples from $10\bar{1}0$ plane of the quartz crystal, one containing fossil tracks and other containing fresh induced tracks (Fig. 5) were taken and etched simultaneously for 12 hrs in 15 N KOH at 125°C. The angular distribution of fossil and induced tracks was obtained by measuring the inclinations of the ends of the tracks relative to c-axis direction (Khan, 1977) in the horizontal plane. These measurements were taken with the help of protractor eye piece provided with the microscope (Fig. 6). Another two samples of the same plane, one containing fossil tracks and the other containing fresh induced tracks, were heated at 750°C for 1 hr and etched simultaneously for 12 hrs in 15 N KOH at 125°C. The angular distribution of these tracks were measured as earlier and is shown in Fig. 6.

6. Track annealing studies and activation energy:

The annealing experiments were carried out to study the effect of temperature on the track annealing rate, V_a, for different planes of quartz. The samples from each plane of the crystal were exposed to ^{252}Cf fission fragments at 15 ± 2° angle of

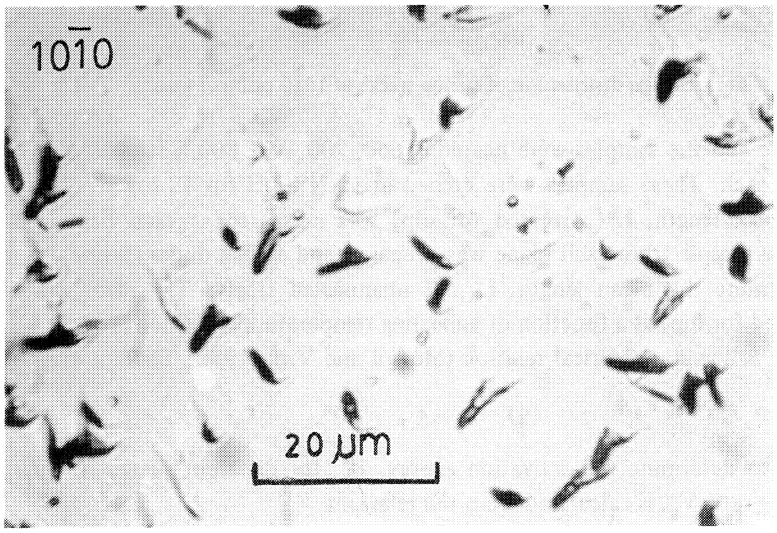

FIG. 5. Micro-photograph of induced fission tracks in quartz.

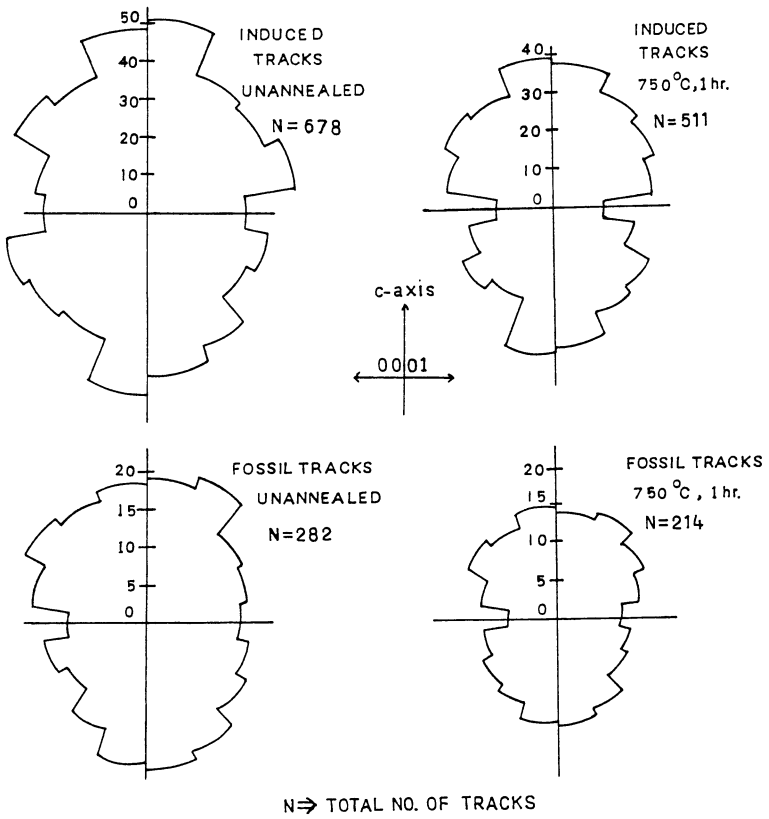

FIG. 6. Angular distribution of fission tracks in $10\bar{1}0$ plane of quartz.

incidence and the samples were heated at 650, 700, 750, 800, 850, 900 and 950°C for 10 min each. These samples were etched in 15 N KOH for 12 hrs at 125°C and the mean track length, L (corrected for dip) was measured at each heating event. A reference sample from each plane was prepared and etched under identical conditions to determine the mean length, L_o, of unannealed tracks. The mean track length (corrected for dip) as a function of annealing temperature is plotted (Fig. 7).

The following empirical relation (Modgil and Virk, 1985., Sandhu *et al.*, 1987b):

$$V_a = A\, t^{-n}\, e^{-E_a/kT} \qquad (4)$$

is used to determine the activation energy, E_a, for different planes of quartz. The annealing rate, V_a, is calculated from the relations

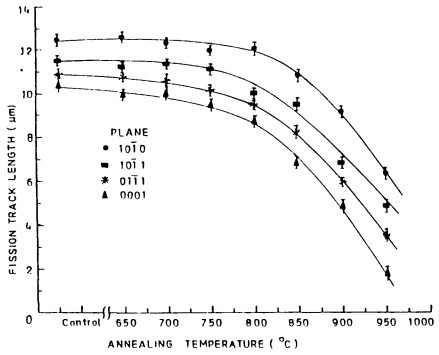

FIG. 7. The variation of mean track length (corrected for dip) with annealing temperature in quartz for heating time of 10 min each.

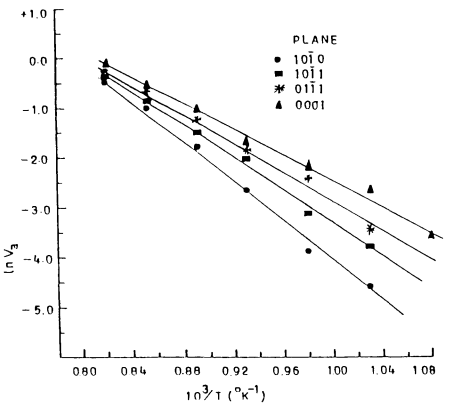

FIG. 8. Plot of ln V_a vs 1/T for different planes of quartz.

$$V_a = (L_o - L)/t \qquad (5)$$

assuming that V_a remains constant over the first 10 min of heating. Here t is the annealing time and k is the Boltzman constant. Plot of ln V_a vs 1/T for different planes is shown in Fig. 8. The activation energies are calculated and are given in Table 1.

7. Age determination of different planes of quartz crystal:

The fission track method of age determination involves the sample preparation, thermal neutron irradiation, etching and scanning of the samples. In the present work the re-etch method (Hurford and Green, 1982) has been used for age determination. The etching of the samples was done in 15 N KOH for 12 hrs. at 125°C. The re-etch method involves counting the spontaneous tracks (due to spontaneous fission of ^{238}U) on an internal surface of each plane of quartz and then re-etching the same surface of each plane for induced tracks (due to induced fission of ^{235}U) after a thermal neutron irradiation (0.41×10^{17} ncm^{-2}). The thermal neutron irradiations of the samples were performed at Bhabha Atomic Research Centre, Bombay., alongwith the standard glass dosimeter (SRM 614). The thermal neutron fluence was calculated from the track density measured in the glass dosimeter.

The fission track age (T) was calculated from the following standard age equation (Price and Walker, 1963., Sandhu *et al.*, 1986):

$$T = 6.45 \times 10^9 \ln (1+9.30 \times 10^{-18} \times \frac{\rho_s}{\rho_i} \times \phi) \qquad (6)$$

where ρ_s = fossil track density
ρ_i = induced track density
and ϕ = thermal neutron fluence (0.41×10^{17} ncm^{-2}).

The results for fission track age determined on different planes equation (6) are given in Table 2 (a,b).

Results and discussion

The fission track density on all the planes of quartz initially increases and becomes constant with increase of etching time (Fig. 1). The track density upto the plateau part increases as a result of very small features originally imperceptible and thence becoming enlarged and visible with increase in etching time. It has been observed that the optimum etch time for revealing maximum tracks varies from plane to plane. It is clear from Fig. 1 that in plane $10\bar{1}0$ the maximum track density is revealed at etching times 6-8 hrs, but in plane 0001 the maximum track density is

TABLE 2(a) Fission track age of quartz crystal.
Thermal neutron fluence (ϕ) = 0.41×10^{17} ncm^{-2}
No. of tracks counted in glass dosimeter (SRM 614) = 400.

	$10\bar{1}0$ plane			$10\bar{1}1$ plane		
Sample No.	ρ_s (x10^2) Tracks cm^{-2}	ρ_i (x10^4) Tracks cm^{-2}	T $\pm$ 1σ Ma	ρ_s(x10^2) Tracks cm^{-2}	ρ_i (x10^4) Tracks cm^{-2}	T $\pm$ 1σ Ma
1.	2.59 $\pm$0.29 (81)*	1.54 $\pm$0.07 (480)	41.2 $\pm$0.53**	2.57 $\pm$0.29 (80)	1.52 $\pm$0.07 (476)	41.5 $\pm$0.50
2.	2.53 $\pm$0.28 (79)	1.52 $\pm$0.07 (475)	40.8 $\pm$0.53	2.58 $\pm$0.29 (81)	1.53 $\pm$0.07 (477)	39.8 $\pm$0.50
3.	2.56 $\pm$0.29 (80)	1.53 $\pm$0.07 (477)	41.0 $\pm$0.53	2.56 $\pm$0.29 (80)	1.59 $\pm$0.07 (496)	39.5 $\pm$0.50
4.	2.43 $\pm$0.28 (76)	1.49 $\pm$0.07 (468)	39.9 $\pm$0.53	2.58 $\pm$0.29 (81)	1.56 $\pm$0.07 (488)	40.5 $\pm$0.50
			Mean 40.73 $\pm$0.27			Mean 40.3 $\pm$0.25

* No. of track counted

** Estimated standard deviation, $1\sigma = \sqrt{\sigma_s^2 + \sigma_i^2 + \sigma_d^2}$

where $\sigma_s = \frac{100}{\sqrt{N_s}}$, $\sigma_i = \frac{100}{\sqrt{N_i}}$, $\sigma_d = \frac{100}{\sqrt{N_d}}$

TABLE 2(b) Fission track age of quartz crystal.
Thermal neutron fluence (ϕ) = 0.41×10^{17} n cm^{-2}
No. of tracks counted in glass dosimeter (SRM 614) = 400.

	$01\bar{1}1$			0001		
Sample No.	ρ_s ($\times 10^2$) Track cm^{-2}	ρ_i ($\times 10^4$) Tracks cm^{-2}	T $\pm 1\sigma$ Ma	ρ_s (10^2) Tracks cm^{-2}	ρ_i ($\times 10^4$) Tracks cm^{-2}	T $\pm 1\sigma$ Ma
1.	2.58 ±0.29 (81)*	1.51 ±0.07 (472)	41.90 ±0.50**	2.43 ±0.28 (76)	1.42 ±0.07 (443)	41.90 ±0.60
2.	2.56 ±0.29 (80)	1.57 ±0.07 (491)	39.90 ±0.50	2.39 ±0.28 (75)	1.41 ±0.07 (441)	41.50 ±0.60
3.	2.58 ±0.29 (81)	1.56 ±0.07 (488)	40.50 ±0.50	2.45 ±0.28 (77)	1.44 ±0.07 (450)	41.70 ±0.60
4.	2.57 ±0.29 (81)	1.61 ±0.07 (493)	39.10 ±0.50	2.41 ± 0.28 (75)	1.43 ±0.07 (444)	41.30 ±0.60
		Mean	40.40 ±0.25		Mean	41.60 ±0.30

* No. of tracks counted

** Estimated standard deviation, $1\sigma = \sqrt{\sigma_s^2 + \sigma_i^2 + \sigma_d^2}$

where $\sigma_s = \frac{100}{\sqrt{N_s}}$, $\sigma_i = \frac{100}{\sqrt{N_i}}$, $\sigma_d = \frac{100}{\sqrt{N_d}}$

achieved at etching time 10-12 hrs. It is also clear from Fig. 1, that the maximum track density, in all the planes can be revealed at etching times 10-12 hrs. This etching time is the optimum etching time. At this optimum etching time the difference in track densities in different planes is minimum. The difference in track densities in different planes may be due to different etching efficiencies. The plane $10\bar{1}0$ shows higher track etching efficiency as compared to the other planes in quartz.

From Table 1, it is evident that V_T, V_G, η and θ_c vary with the crystallographic orientations. This shows that the track etching behaviour of quartz is anisotropic. The value of V_T varies from 1.1 μm/hr for 0001 plane to a maximum of 2.7 μm/hr for $10\bar{1}0$ plane. Similarly, V_G varies from 0.11 μm/hr for 0001 plane to 0.16 μm/hr for $10\bar{1}0$ plane. The etching efficiency varies from 90 to 94.1% and critical angle varies from 5.7 to 3.4° on corresponding planes. Also it is evident from Fig. 2 that maximum etchable range of ^{252}Cf fission tracks varies from plane to plane, being maximum in $10\bar{1}0$ plane (12.8 μm) and least in 0001 plane (10.3 μm). It is evident from Table 1 that the value of activation energy for track etching varies from 0.143 eV for $10\bar{1}0$

plane to 0.221 eV for 0001 plane. This shows that fission tracks in $10\bar{1}0$ plane of quartz can be easily etched compared to other planes of the crystal. Fig. 6 shows the angular distribution of the etched induced and fossil tracks in $10\bar{1}0$ plane. The distribution of both type of tracks is anisotropic. More tracks are lying parallel or nearly parallel to c-axis of the crystal. The degree of anisotropy is increased when the induced and fossil tracks are subjected to annealing. However, the difference of angular distribution of fresh induced and fossil tracks in quartz is small as compared to the results reported in apatite (Sandhu et al., 1987a). The reason for this is that the fission fragment tracks in quartz are less sensitive to thermal effects as compared to apatite. It is clear from Fig. 6 that annealing augments the anisotropy of track revelation in quartz, as was observed in apatite (Sandhu *et al.*, 1987 a).

Also the annealing of fission tracks occurs faster (Fig. 7) for samples cut perpendicular to c-axis (0001 plane) than for ones cut parallel ($10\bar{1}0$ plane). Since the annealing is a diffusion of interstitial atoms and atomic vacancies, it must be a function of spacing between different planes. The value of activation energy, E_a, for track annealing in $10\bar{1}0$ plane (Table 1) is higher (1.73 eV) than in 0001 plane (1.15 eV). This indicates that the interstitial atoms require less amount of energy to start the process of annealing in a plane perpendicular to c-axis. The difference in E_a may be due to different total point defect concentration in different orientations. These results corroborate with our earlier findings for apatite (Sandhu *et al.*, 1987 a).

The value of F.T. age comes out to be nearly the same (Table 2a, b) for all the planes of quartz. However, it is clear from the Table 2 (a, b) that $10\bar{1}0$ plane shows higher value of ρ_i and ρ_s as compared to 0001 plane. This is due to the higher etching efficiency of $10\bar{1}0$ plane. Since F.T. age is determined by the ratio of ρ_s to ρ_i, the effect of anisotropy is negligible, if the fossil and induced tracks are counted in the same sample (re-etch method).

Conclusions

1. Etching characteristics of fission tracks in quartz are anisotropic.
2. The annealing of fission tracks increases the degree of anisotropy.
3. F.T. age is nearly same on all planes of quartz crystal.
4. The plane $10\bar{1}0$ (parallel to c-axis) is found to be most suitable for fission track dating purposes.

Acknowledgements–The authors are thankful to Dr. N.P. Singh for providing the quartz crystal. They are also thankful to Mr. Jagmohan Singh for help in preparation of the samples. One of the authors (A.S. Sandhu) is thankful to the Council of Scientific and Industrial Research (CSIR), New Delhi, for providing him with a Senior Research Fellowship.

References

DAVIE, I.W. and DURRANI, S.A. (1978) *Nucl. Tracks* **2,** 199-205.
DURRANI, S.A., KHAN, H.A. BULL, R.K., DORLING, G.W. and FREMLIN, J.H. (1974). *Proc. 5th Lunar Sci. Conf., Geochim. Cosmochim Acta Suppl.,* **5,** 2543-2560.
FLEISCHER, R.L., PRICE, P.B. and WALKER, R.M. (1975) *Nuclear Tracks in Solids, Principles and Applications,* University of California Press, Barkeley, U.S.A.
FRONDEL C. (1962) *The System of Mineralogy,* John Wiley Inc. New York Vol III (silica minerals) 116-117.
GEGUGIN, Ya. E., VOREBEVA, I.V. and BERZINA, I.G. (1968) *Soviet Physics-Solid State* **10,** 1431-1433.
GLEADOW, A.J.W. (1978) *Nucl. Tracks* **2,** 105-117.
GREEN, P.F. and DURRANI, S.A. (1977) *Nucl. Tracks* **1,** 33-39.
HURFORD, A.J. and GREEN, P.F. (1982) *Earth. Planet. Sci. Lett.* **59,** 342-354.
KHAN, H.A. (1977) *Radiat. Effects* **32,** 49-53.
MODGIL, S.K. and VIRK, H.S. (1985) *Nucl. Instrum. Meth. Phy. Res.* **B 12,** 212-218.
PRICE, P.B. and WALKER, R.M. (1963) *J. Geophys. Res.* **68,** 4847-4862.
SANDHU, A.S., SINGH,S. and VIRK, H.S. (1986) *Mineral. Journ.* **13,** 177-186.
SANDHU, A.S.,SINGH, S. and VIRK, H.S. (1987a) *Mineral. Journ.* **13,** 307-313.
SANDHU, A.S., SINGH, S. and VIRK H.S. (1987b) *Mineral. Journ.* **13,** 254-259.
SINGH, N.P. SINGH, M. SINGH, S. and VIRK, H.S. (1984) *Nucl. Tracks* **8,** 41-44.
SINGH, S. SINGH, D. SANDHU, A.S. and VIRK, H.S. (1986) *Mineral Journ.* **13,** 75-85.

Received April 13, 1987; revised August 24, 1987.